

# Interferometric calibration of rotary axes

by M.A.V. Chapman, A. Holloway, W. Lee, M. May, S. McFadden, D. Wall

## Introduction

This paper describes the operational principles behind Renishaw’s XR20 rotary axis calibration system and how it can be used ‘on axis’ to calibrate axes of rotation. It examines the various error sources that affect the accuracy of measurement and describes how the system has been designed, and should be used, in order to minimise such errors. It concludes with a section describing how the XR20 system can be used ‘off axis’ to calibrate 4th and 5th axes on CNC machines.

## Interferometric angular measurement

Figure 1 illustrates the use of a laser and angular interferometer to measure small angles of rotation of a rotary axis. As the axis rotates, the laser system detects the relative change between the optical path lengths in the two “arms” of the interferometer. As the axis rotates by angle  $\theta$ , the laser beam in Arm 1 will get shorter by  $S \cdot \sin(\theta)$  and the laser beam in Arm 2 will get longer by  $S \cdot \sin(\theta)$  where  $S$  is the separation between the two retro-reflectors. The total relative change in the path lengths, between Arms 1 and 2 of the interferometer, is therefore  $2S \cdot \sin(\theta)$ . This change in path lengths is detected by an interference fringe counter/interpolator inside the laser’s detector unit. The resulting fringe count is converted into a linear distance,  $\Delta L$ , by multiplying by the laser wavelength/2.

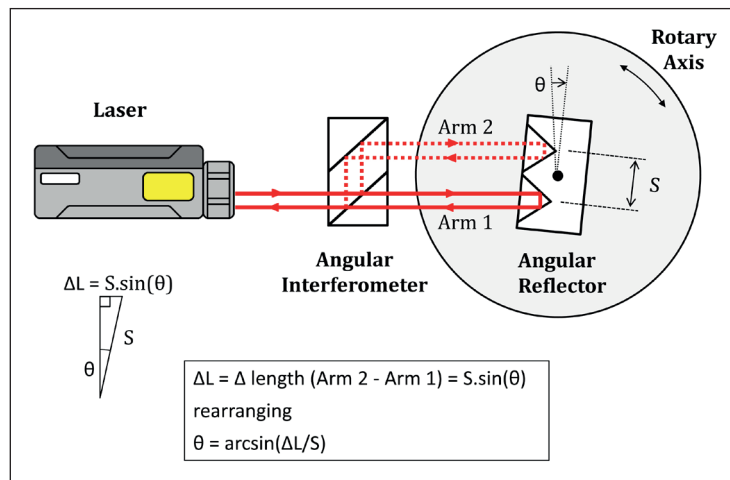


Figure 1

The resulting fringe count is converted into a linear distance,  $\Delta L$ , by multiplying by the laser wavelength/2.

$$\Delta L = \text{Fringe count} \times \text{laser wavelength} / 2$$

In angular mode the laser system software then converts  $\Delta L$  into an angular measurement by calculating  $\arcsin(\Delta L/S)$ .

$$\theta = \arcsin(\Delta L/S)$$

For a more detailed explanation of angular interferometry, please refer to the Renishaw White Paper entitled ‘TE326 - Interferometric angle measurement and the hardware options available from Renishaw’.

## Rotary axis calibration

The arrangement shown in Figure 1 is only suitable for checking angular movements over a range of about  $\pm 10^\circ$  because, at larger angles, the rotation of the angular reflector will cause misalignment of the returned laser beams and a corresponding loss of signal strength.

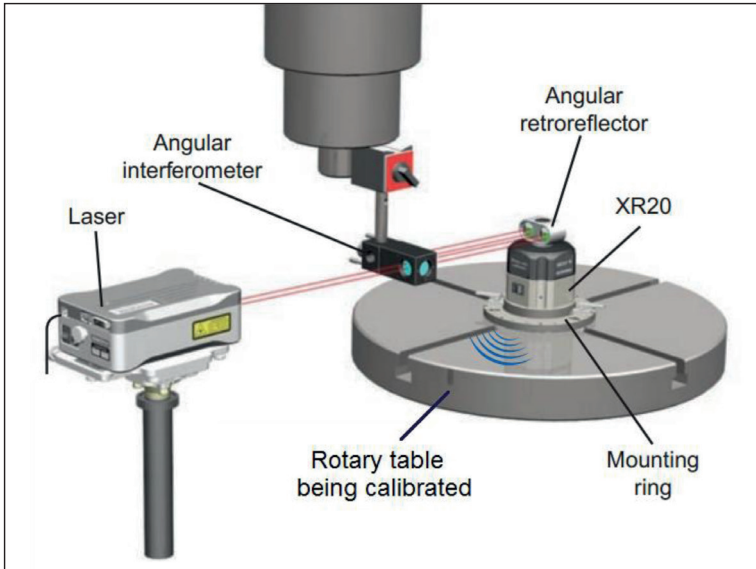


Figure 2

However, this limitation can be readily overcome by combining measurements from the laser interferometer with those from a high accuracy rotary axis, such as Renishaw's XR20. A typical setup is shown in Figure 2. An angular reflector is mounted on top of the XR20, which in turn is mounted on top of the rotary axis being calibrated. As the axis under test is rotated from one target position to the next, the XR20 is driven in the opposite direction in order to maintain alignment of the angular interferometer. When the axis under test stops at each target position, the positioning error is calculated by comparing the target

position with the arithmetic sum of the angular readings from the laser interferometer and the XR20. This allows calibration of the axis over a full 360° or even over multiple revolutions.

A key benefit of using an angular interferometer to provide the 'coupling' between the counter-rotating XR20 and a stationary part of the axis under test, is that it's largely insensitive to small translation (side to side) movements of the reflector. (This topic is covered in the *Operational Principles* section of *TE326*). This makes system alignment much easier by largely eliminating a major potential source of angular measurement error. For example, eccentrically mounting an XR20, 1mm from the centre of rotation of the axis under test, adds less than  $\pm 0.5$  arcseconds of measurement error. For comparison a 200mm diameter rotary encoder disk, with external read-head, would have to be mounted to within  $0.25\mu\text{m}$  to achieve similar performance. Even a fully enclosed rotary encoder with integral bearings and sophisticated precision shaft coupling has to be mounted within about 0.05mm (a 40x tighter tolerance than that required by XR20).

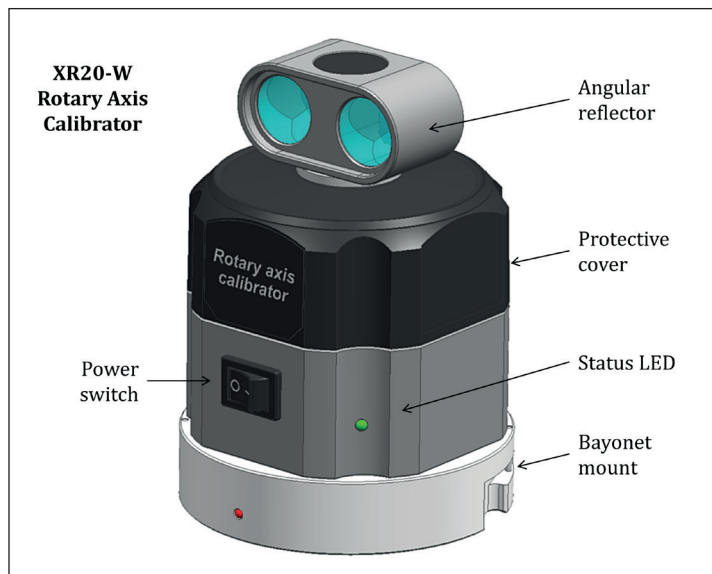


Figure 3

Nevertheless, keeping overall accuracy levels within  $\pm 1$  arcseconds requires careful design and attention to detail to ensure all of the possible error sources are similarly controlled. The following sections give an insight into the internal design of Renishaw's XR20 followed by an analysis of the main error sources associated with the system and its use.

## The XR20 – A closer look

The XR20 is a battery powered, radio controlled, high accuracy servo controlled rotary axis with an angular reflector mounted on a central shaft. Figure 3 shows an external view of the XR20.

The XR20 contains the following items, as shown in the cutaway view in Figure 4, and the simplified cross-section in Figure 5.

- A central shaft on which an angular reflector, rotary encoder and direct drive servo motor are all mounted.
- A high accuracy rotary encoder with two diametrically opposed read-heads and axial encoder graduations which are directly formed on the outer edge of the encoder disk to provide long term stability. The solid aluminium encoder disk's high thermal conductivity, low thermal capacity and thick cross section ensure any temperature changes and resulting expansions/contractions are evenly distributed around the disk thereby minimising local distortions. The diametrically opposed read-heads largely eliminate errors due to eccentricity of the encoder disk relative to the central shaft, or lateral movement due to bearing wander/play. (This is covered in more detail later).
- A low power, direct drive, servo controlled motor to rotate the central shaft. The rotor magnets are bonded directly to the central shaft and the coils to the XR20 body. This motor provides a high resolution, contactless, drive of the central shaft free from friction, backlash and play with minimal power dissipation, thereby maximising battery life. The efficient, low power design also minimises self-heating, and the rotational symmetry helps ensure any heat generated is evenly distributed.

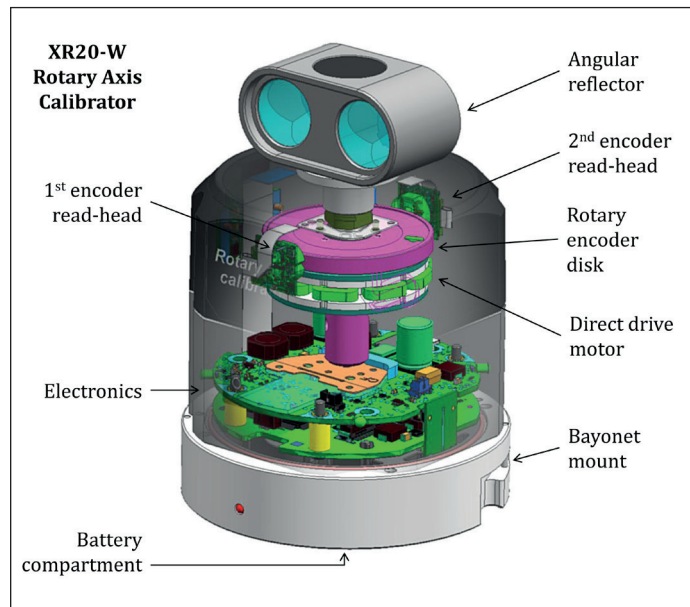


Figure 4

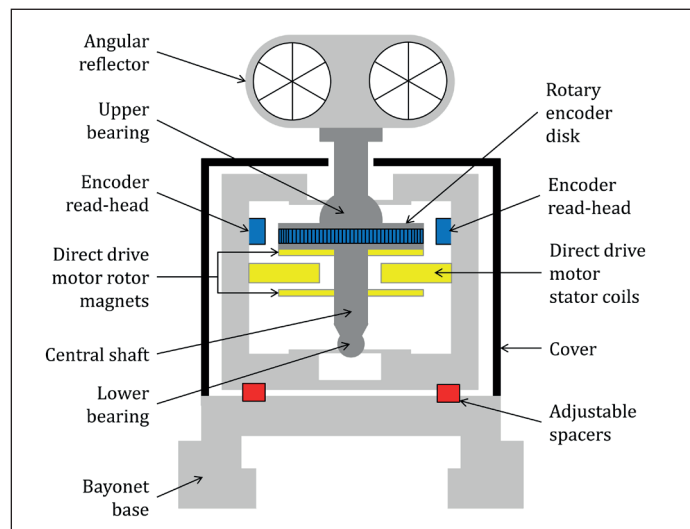


Figure 5

- Adjustable spacers to allow the axis of rotation of the central shaft to be set perpendicular to the mounting surface of the bayonet base.
- Two preloaded, self-centering spherical bearings to minimise eccentricity errors, bearing wander and end-float.
- Sophisticated electronics including; Encoder graduation interpolation circuitry to give 0.1 arcsecond resolution; Automatic balancing/gain control of the encoder read-head signals in order to minimise sub-divisional errors (covered in more detail later), and an integrated encoder error map generated during system manufacture/calibration.
- Home sensor to allow system orientation and error map referencing.

- Bluetooth wireless communications with the PC providing cable free operation, simplifying set-up and avoiding problems with cable drag.
- Interchangeable Lithium Polymer rechargeable battery allowing 3 hours of typical operation between charges.
- Bayonet mount with quick-release clamping to a separate mounting ring to allow easy fitment and removal to a wide variety of rotary axes / tables.

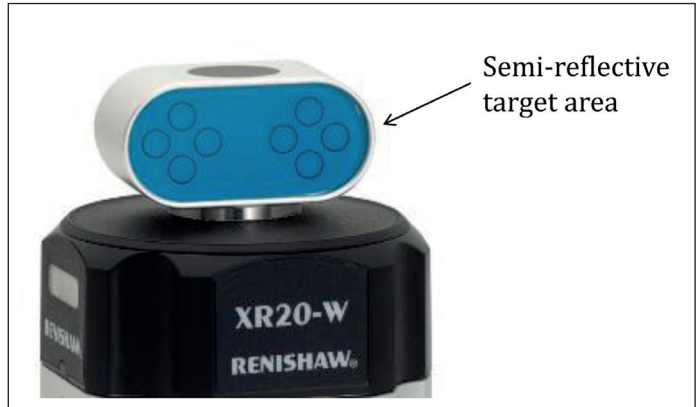


Figure 6

- Semi-reflective target on the rear of the angular reflector to simplify beam alignment (See Figure 6).

## Error analysis

The main sources of error may be broadly divided into 3 categories, namely;

- Errors due to angular misalignment of axes
- Inaccuracies in the rotary encoder reading
- Inaccuracies in the laser interferometer reading

These are discussed in sequence below.

## Errors due to angular misalignment of axes

There are 3 main angular misalignments to consider, as shown in Figure 7

- Angular Misalignment ( $\alpha$ ) between the axes of rotation of the axis under test and the XR20. This typically arises from three sources, the non-perpendicularities of the mounting surfaces of both the axis under test and the XR20 to their respective axes of rotation, and damage or debris on these mounting surfaces.
- Angular misalignment ( $\beta$ ) between the “line of sight” of the laser interferometer and the plane of rotation of the axis under test.
- Angular misalignment ( $\omega$ ) of the centre-line between the two retro-reflectors in the angular reflector and the axis of rotation of XR20. This centre-line should be perpendicular to the axis of rotation.

Some of these misalignments are tightly controlled by Renishaw during the XR20 manufacturing process, others are the responsibility of the user to control during system set-up.

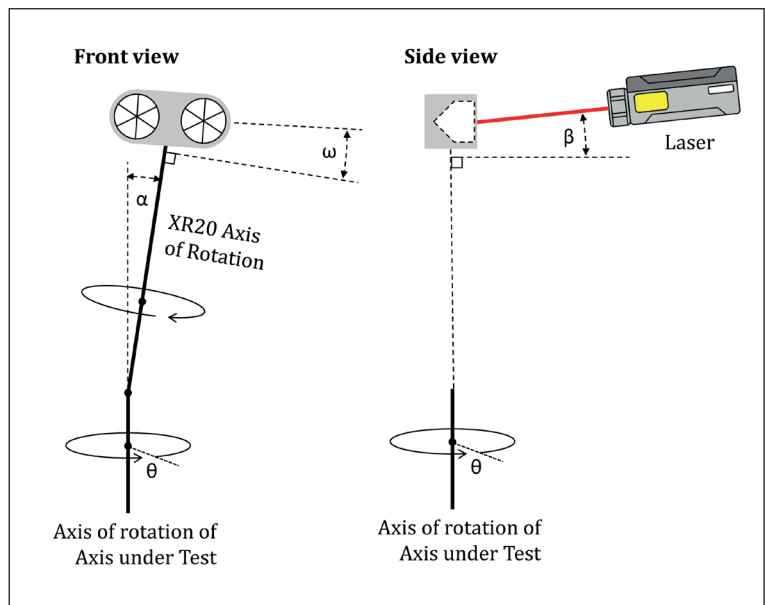


Figure 7

These angular misalignments give rise to a measuring error,  $E_\theta$ , at angle  $\theta$ , of the form;

$$E_\theta = \sin(2\theta) \cdot \alpha^2/4 + \sin(\theta) \cdot \alpha\beta + \cos(\theta) \cdot \alpha\omega \dots\dots\dots (1)$$

*Note: For simplicity, this paper assumes the misalignment angle  $\alpha$  lies in the direction of  $\theta = 0^\circ$ . In reality  $\theta$  should be replaced with  $\theta + \eta$ , where  $\eta$  is an arbitrary angular offset. This doesn't affect the form and magnitude of the induced measurement error (over  $360^\circ$ ), but will vary its phase.*

Looking at Equation 1 it can be seen that the measurement error,  $E_\theta$ , is the sum of three distinct error terms. An  $\alpha^2/4$  based term, an  $\alpha\beta$  term and finally  $\alpha\omega$  based term, where  $\alpha$ ,  $\beta$  and  $\omega$  are misalignment angles in radians. Each term is now examined in detail.

**$\alpha^2/4$  term** - The origin of this term is illustrated by Figures 8, 9 and 10. As the axis under test rotates, the misalignment,  $\alpha$ , between the axes of rotation will cause the axis of rotation of the XR20 to sweep out a cone, as shown (grossly exaggerated) in Figure 8. As the test progresses the XR20 will counter-rotate to ensure the angular reflector remains facing towards the laser. The combined motions will make the angular reflector appear to “wobble”. As seen from the laser, the reflector appears to progress from being tipped slightly forwards (at position 1), then slightly to the right (at position 2), then slightly backwards (at position 3) and to the left (at position 4). Note that, in reality - unlike in Figure 8, the amount of wobble will be tiny, with the reflector only moving a fraction of a millimetre.

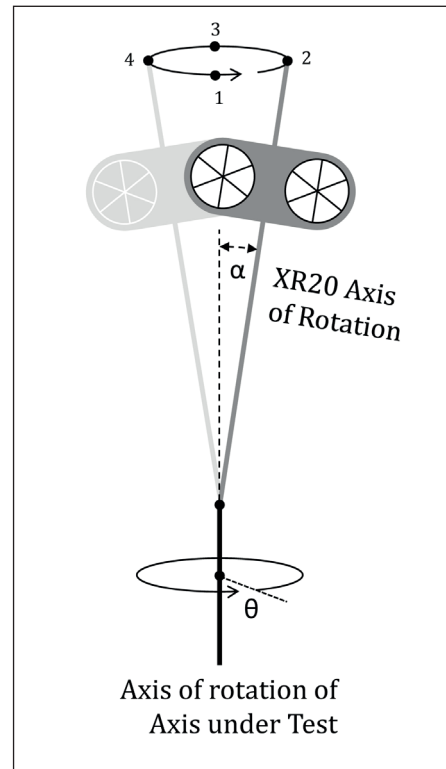


Figure 8

This wobbling motion is illustrated in Figure 9 which shows how the retro-reflectors wobble relative to the laser due to misalignment  $\alpha$  between the axes of rotation, and when misalignments  $\beta$  and  $\omega$  are zero.

As seen from the front (upper row of pictures in Figure 9) the reflector appears to tip from side to side (i.e. roll) by an angle of  $\pm\alpha$ . At any moment during the test the roll angle is given by  $\alpha \cdot \sin\theta$ , where  $\theta$  is the angle of rotation of the axis under test (*assuming  $\eta = 0^\circ$* ).

As seen from the side (lower row of pictures in Figure 9) the reflector appears to tip (i.e. pitch) back and forth by an angle of  $\pm\alpha$ . At any moment during the test the current pitch angle is given by  $\alpha \cdot \cos\theta$ , where  $\theta$  is the angle of rotation of the axis under test (*again assuming  $\eta = 0^\circ$* ).

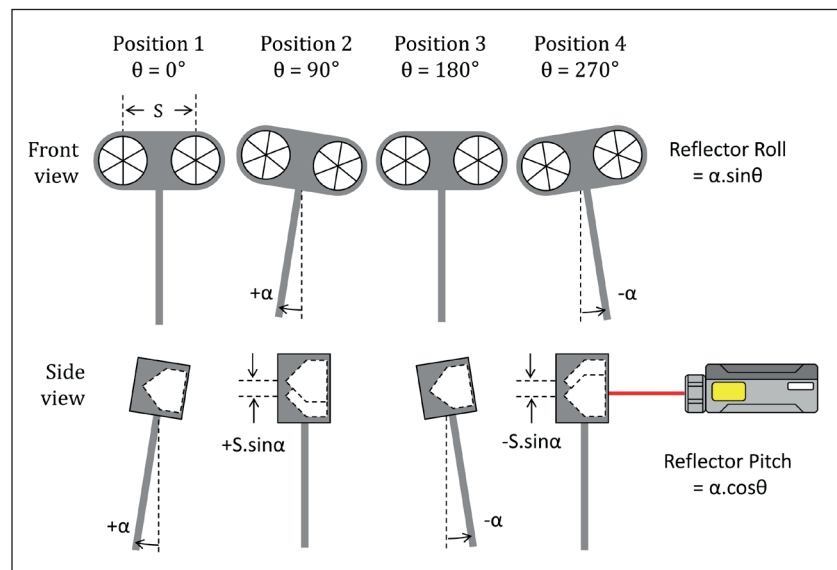


Figure 9

The wobbling motion of the reflector is therefore a combination of roll of  $\alpha \cdot \sin\theta$  and a pitch of  $\alpha \cdot \cos\theta$ . This combination causes the individual reflectors to rise and fall relative to one another, as well as moving

towards and away from the laser. The maximum roll occurs when there is no pitch and vice versa. At positions 2 and 4 the reflectors are at different heights. But, because the reflector is not also tipped forward or backward, their movements are at  $90^\circ$  to laser beam. Therefore, the laser path lengths

to the reflector are unaffected and there is no measurement error at these positions. At positions 1 and 3 the reflectors are tipped forwards or backwards. But, because they are at the same height, no measurement error occurs at these positions either.

However, at intermediate positions a measurement error will occur because here there will be some tipping (pitching) of the reflector whilst the retro-reflectors are also at differing heights.

The difference in retro-reflector height, when the table under test is at an angle  $\theta$ , is given by  $S.\alpha.\sin\theta$  and the reflector pitch angle is  $\alpha.\cos\theta$ . This combination will give a change in the relative laser path lengths in the two arms of the interferometer of  $S.\alpha.\sin\theta.\alpha.\cos\theta$  or  $S.\alpha^2.\sin\theta.\cos\theta$ . Dividing by  $S$  and substituting  $2.\sin\theta.\cos\theta = \sin(2\theta)$  gives an angular measurement error of  $\alpha^2.\sin(2\theta) / 2$ . This result is similar to the 1st term in Equation 1, but has twice the amplitude.

To understand why the amplitude is halved, we must also consider the variation in yaw\* angle of the reflector due to the misalignment,  $\alpha$ , between the axes. \*Yaw is defined as rotation of the reflector about the axis under test. As the axis under test rotates through an angle  $\theta$ , the XR20 will counter-rotate by  $-\theta$ . However, because the axes are misaligned by an angle  $\alpha$ , these rotations will not exactly cancel producing a small yaw error in the angle of the reflector. This is illustrated in Figure 10.

Imagine the two planes of rotation are represented by two disks of unity radius. The axis under test is shown in blue. The XR20 is shown in red misaligned by an angle of  $\alpha$  (shown grossly exaggerated in the figure). Looking from above (directly along the test axis of rotation) the test axis (in blue) appears as a perfect circle. But the XR20 (in red) appears as an ellipse. If both axes rotate by  $0^\circ$ ,  $90^\circ$ ,  $180^\circ$  or  $270^\circ$ . Their angles of rotation, as seen from above, appear identical. However, at intermediate angles this is not true, as illustrated by triangle ABC.

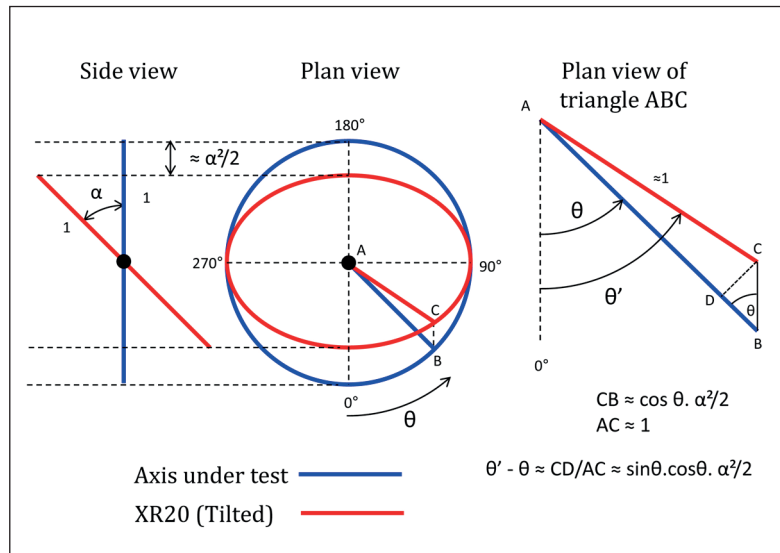


Figure 10

If both axes rotate by an angle  $\theta$

then, looking down from directly above, the axis under test (blue) will appear to rotate by  $\theta$ , but the XR20 (red) will appear to rotate by  $\theta'$ . Looking at the plan view and using small angle approximations it can be seen that length  $CB \approx \cos\theta. \alpha^2/2$ . Looking at triangles ABC and BCD, it can be seen that  $CD = CB.\sin\theta$ , so  $CD \approx \sin\theta.\cos\theta. \alpha^2/2$ . Also, the difference in angle  $\theta' - \theta \approx CD/AC$ , where  $AC \approx 1$ , so  $\theta' - \theta \approx \sin\theta.\cos\theta. \alpha^2/2$ . This can be simplified using the trig identity  $\sin\theta.\cos\theta = \frac{1}{2} \sin 2\theta$  to give the final result;

$$\text{Reflector yaw} = (\theta' - \theta) \approx \sin 2\theta. \alpha^2/4$$

Inspection shows that the resulting measurement error has the opposite sign to that caused by pitch and roll of the reflector described earlier. Therefore combining the effects of reflector pitch and roll (from the optics wobble), with reflector yaw produces a measurement error of:-

$$\alpha^2.\sin(2\theta) / 2 - \alpha^2.\sin(2\theta) / 4 = \alpha^2.\sin(2\theta) / 4$$

This explains the 1st term in Equation 1.

Figure 11 shows the form of this measurement error for angular misalignments of  $\alpha = 0.1^\circ$ ,  $0.25^\circ$  and  $0.5^\circ$ . Note, although the form of this error always contains 2 cycles over  $360^\circ$ , the phase may be completely different depending on  $\eta$ . The graph indicates the axes of rotation must be aligned to better than  $\pm 0.2^\circ$  to reduce the measurement error contribution, from this term alone, to below  $\pm 1$  arcsecond. The XR20 contains spacers (see Figure 5) which are adjusted during manufacture to ensure the XR20's axis of rotation is perpendicular to its mounting face to within  $\pm 0.025^\circ$ . It is also important that the XR20 is mounted on a surface that is sufficiently perpendicular to the axis of rotation of the axis under test. This can be verified by indicating the XR20's mounting ring with a dial gauge whilst rotating the test axis. To achieve an overall measurement accuracy of  $\pm 1$  arcsecond, the XR20 manual recommends that the TIR should be  $< 0.04\text{mm}$  at  $50\text{mm}$  radius ( $0.025^\circ$ ). Thereby ensuring the total  $\alpha$  will be less than  $\pm 0.05^\circ$ .

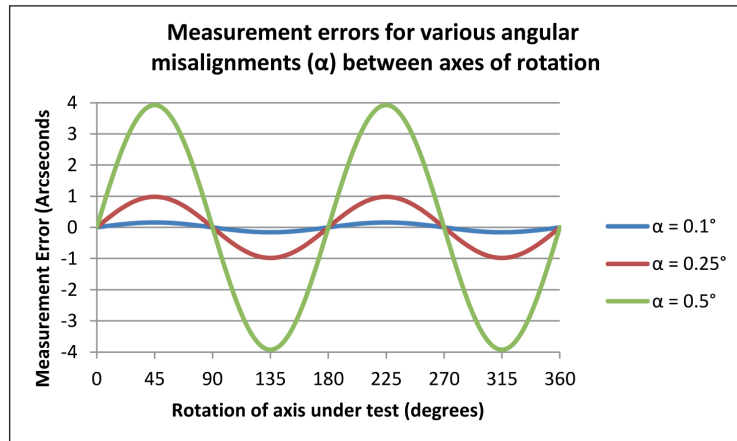


Figure 11

The origin of the second and third terms,  $\sin(\theta).\alpha\beta$  and  $\cos(\theta).\alpha\omega$  in Equation 1, depends on the presence of two or more misalignment errors at the same time. There must be a misalignment ( $\alpha$ ) between the axes of rotation in combination with some misalignment ( $\beta$ ) of the laser and/or some misalignment ( $\omega$ ) of the reflector optics.

**$\alpha\beta$  term** - Consider what happens when, in addition to a misalignment ( $\alpha$ ) between the axes of rotation, the 'line of sight' of the laser is also misaligned by an angle  $\beta$  to the plane of rotation of the axis under test (refer to Figure 7). This additional misalignment alters the effect of the wobble of the angular reflector, as illustrated in Figure 12.

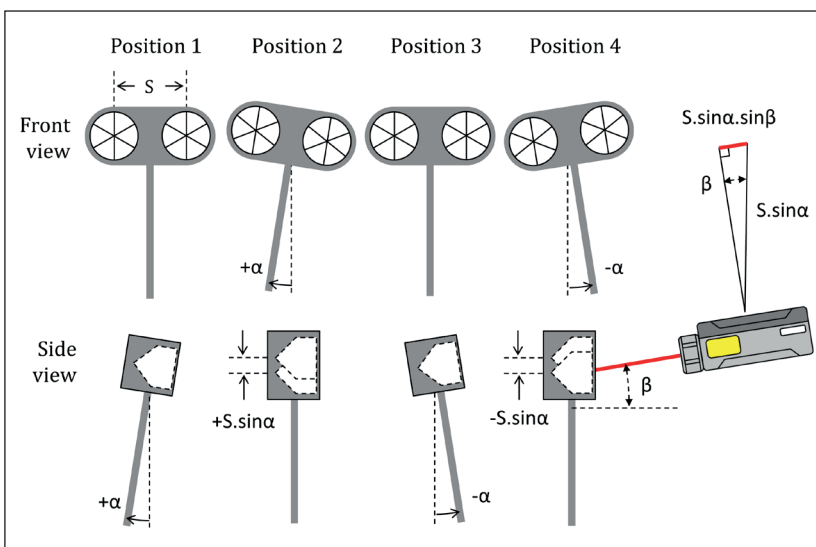


Figure 12

Previously, when the laser was correctly aligned ( $\beta = 0^\circ$ ), the side to side tipping (rolling) of the reflector at positions 2 and 4 didn't introduce any measurement error because the movement of the reflectors was at  $90^\circ$  to the laser beam.

However, if the laser is misaligned by an angle  $\beta$ , then Arms 1 and 2 of the interferometer will detect a small resolved component ( $\Delta L = \pm S.\sin\alpha.\sin\beta$ ) of the differential movement between the retro-reflectors. The laser system software will convert

this into an angular measurement by calculating  $\theta = \arcsin(\Delta L/S)$ , where  $S$  is the retro-reflector separation. Thereby producing an additional variation in the angular reading of  $\pm\alpha.\beta$  if  $\alpha$  and  $\beta$  are expressed in radians.

If  $\theta = 0^\circ$  is defined as being at position 1, (i.e.  $\eta = 0$ ), the equation of the induced measurement error is  $\sin(\theta).\alpha.\beta$ . This explains the second term in Equation 1 above.

In order to help align the laser and thereby control the value of  $\beta$ , the XR20 contains a reflective target on the back of the angular reflector which is aligned to the XR20's axis of rotation to within  $\pm 0.33$  milliradians. The XR20 manual recommends that, if the laser is placed 1 metre away from the XR20, the reflected return beam is aligned to within 1mm on the laser shutter. This will ensure the laser is aligned within  $\pm 0.5$  milliradians to the reflective target, which in turn (allowing for other errors) will ensure  $\beta$  is less than 1 milliradian.

*Note: The effect of various combinations of misalignment errors on measurement accuracy are presented in the table in Figure 22, towards the end of this paper.*

**$\omega$  term** - Finally, consider what happens if, instead of the laser being inclined at an angle of  $\beta$ , the angular reflector is twisted by an angle of  $\omega$ . This is illustrated in Figure 13 (note that Position 1 now appears on the right).

Previously, when the reflector wasn't twisted, ( $\omega = 0^\circ$ ), the forward and backward pitching of the reflector at positions 1 and 3 didn't introduce any measurement error because the reflectors were at the same height.

However, if the reflector is twisted by  $\omega$ , this is no longer true. Comparing positions 1 and 3 it can be seen that the upper retro-reflector now moves back and forth in the direction of the laser relative to the lower retro-reflector. The amount of differential movement is given by  $\Delta L = \pm S \cdot \sin \omega \cdot \sin \alpha$ . The laser system will convert this into an angular reading by calculating  $\theta = \arcsin(\Delta L/S)$ , where  $S$  is the retro-reflector separation. This will produce an additional variation in the angular reading of  $\theta \approx \pm \sin \alpha \cdot \sin \omega$  if  $\alpha$  and  $\beta$  are expressed in radians. At positions 2 and 4, although the height of the retro-reflectors still varies (by the same amount as in Figure 12), this movement is now at right angles to the laser beam, so there's no measurement error at these positions.

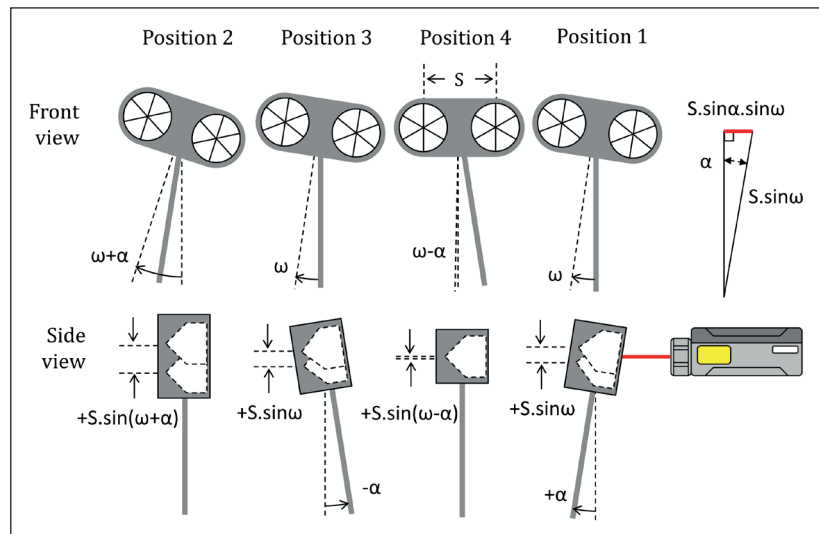


Figure 13

The amount of differential movement is given by  $\Delta L = \pm S \cdot \sin \omega \cdot \sin \alpha$ . The laser system will convert this into an angular reading by calculating  $\theta = \arcsin(\Delta L/S)$ , where  $S$  is the retro-reflector separation. This will produce an additional variation in the angular reading of  $\theta \approx \pm \sin \alpha \cdot \sin \omega$  if  $\alpha$  and  $\beta$  are expressed in radians. At positions 2 and 4, although the height of the retro-reflectors still varies (by the same amount as in Figure 12), this movement is now at right angles to the laser beam, so there's no measurement error at these positions.

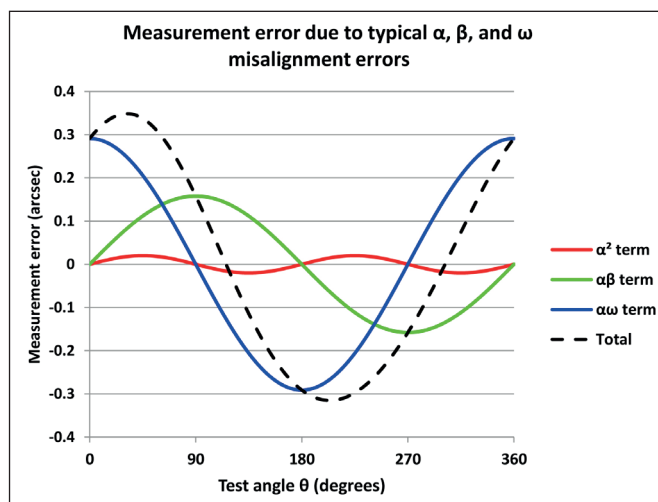


Figure 14

If  $\theta = 0^\circ$  is again defined as being at position 1, the equation of the induced measurement error is  $\cos(\theta) \cdot \alpha \cdot \omega$ . This explains the 3rd term in Equation 1 above.

The alignment of the retro-reflectors and reflector housing are set during XR20 manufacture to be within  $\pm 2.5$  milliradians.

**Combined error** – Figure 14 shows an example of the error profile produced by combining XR20 manufacturing tolerances with recommended system alignment values (giving  $\alpha = 0.62$ ,  $\beta = 1.23$  and  $\omega = 2.26$  milliradians), and then substituting into Equation 1.

*Note: The effects of various combinations of  $\alpha$  and  $\beta$  misalignments on overall measurement accuracy are presented in the table in Figure 22, towards the end of this paper.*



## Inaccuracies in the rotary encoder reading

There are three main sources of error associated with the rotary encoder reading.

- Sub-divisional errors within the interpolation system
- Bearing wander and eccentricity of the encoder disk
- Inaccuracies in the positions of the graduations formed on the periphery of the encoder disk

These errors and their control are discussed in more detail below.

### Sub-divisional errors

Renishaw's in house rotary encoder manufacturing process produces a total of 7,850 graduations at 20 μm intervals around the periphery of the XR20's 50mm diameter encoder disk. Giving an effective angular interval, between graduations, of 165 arcseconds.

In order to increase the resolution, the XR20 system uses a sophisticated interpolation system to sub-divide each angular interval by 2000x to give an angular resolution of ~0.08 arcseconds. As the encoder disk rotates, the graduations will move past the read-head, causing the photo-detectors inside the read-head to detect sinusoidal variations in the light levels falling on them. The photo-detectors are arranged so that their phases are offset by 90°, and so produce sine and cosine output signals as shown in

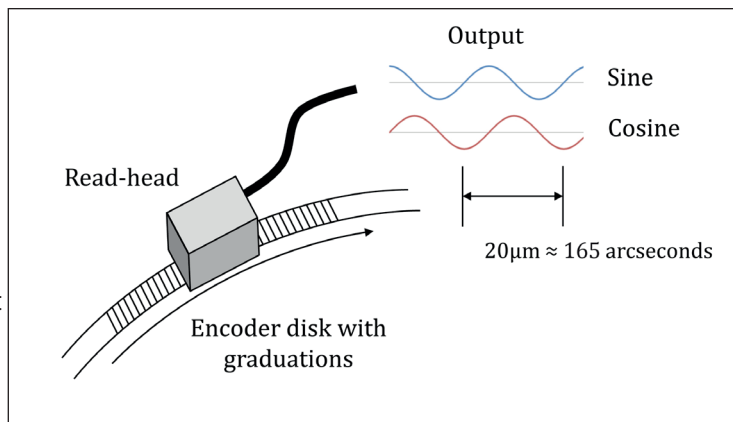


Figure 15

Figure 15. These signals are fed to electronic circuitry which counts the number of cycles of the sine or cosine signal to give a coarse angular position, to the nearest 165 arcseconds. The electronics also interpolates within each cycle to give the fine resolution. If the sine and cosine signals are plotted on the X and Y axes of a graph, a circular “lissajous” figure appears (see Figure 16). The plotted signals complete one revolution of the lissajous figure each time an encoder graduation passes in front of the read-head, (which occurs every time the XR20 rotates by 165 arcseconds).

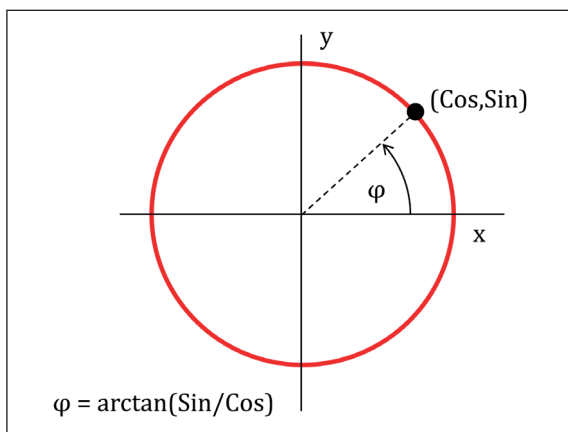


Figure 16

Interpolation is carried out by digitising the signals to give instantaneous values for sine and cosine and then digitally calculating the phase angle,  $\phi$ , by computing  $\phi = \arctan(\sin/\cos)$ . The fine angle position of the XR20 in arcseconds is then calculated from  $\phi \cdot 165/360$ , and this is added to the coarse position to give an overall angular position value.

This interpolation process works well if the sine and cosine signals are perfect. However, if they are not perfect the lissajous will be distorted and a sub-divisional error (SDE) will be introduced. The electronic circuitry within the XR20 is designed to minimise the SDE error as follows;

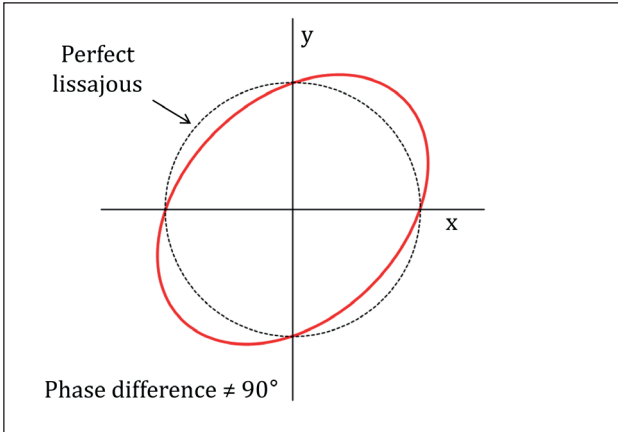


Figure 17

Firstly, due to optical and mechanical tolerances between the read-head and encoder graduations, the phase difference between the photo-detector signals may not be exactly 90°. This can cause a distorted lissajous, as shown in Figure 17. This error is removed during manufacture firstly by mechanical adjustment and then by electronically mixing a small proportion of the inverted signal from one photo-detector with another, to adjust the phase to 90°.

Secondly, the amplitudes of the photo-detector signals may not be correct. This can cause a distorted lissajous as shown in Figure 18. This error is removed electronically as follows; The XR20 constantly monitors the amplitudes of the sine and cosine signals. Errors are corrected by adjusting the intensity of the LED (which illuminates the encoder graduations) and by using ABC (automatic balance control) circuitry, to ensure the both signals are balanced and of the correct amplitude.

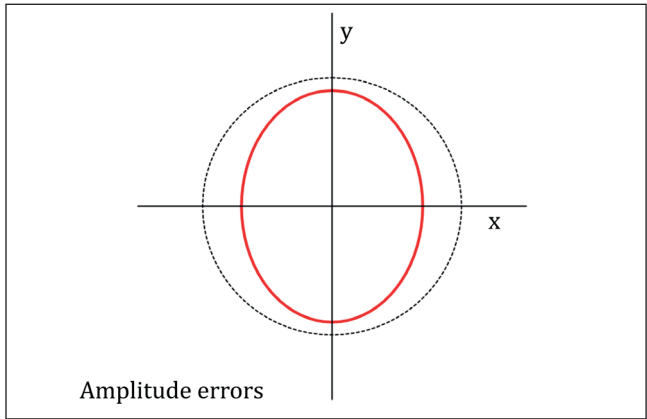


Figure 18

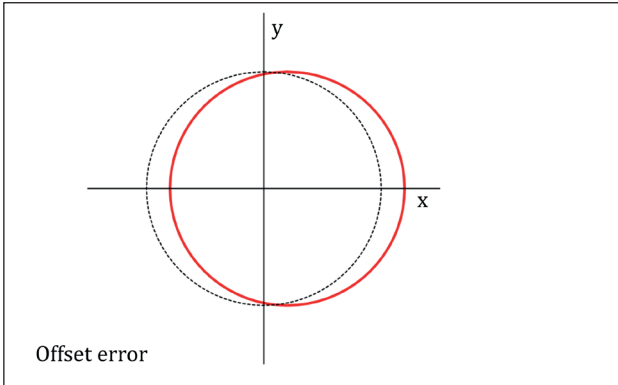


Figure 19

Finally, there may be a DC offset in one or more of the signals which can cause a distorted lissajous as shown in Figure 19. This error is also removed electronically as follows; The XR20 constantly monitors the DC offsets of the sine and cosine signals and uses AOC (automatic offset control) circuitry to remove any offsets.

These error corrections ensure that the sub-divisional error is kept below  $\pm 0.25$  arcseconds.

## Bearing wander and encoder mounting eccentricity

There is likely to be some radial wander in the bearings supporting the XR20's central shaft and encoder disk. This will allow the encoder disk to move sideways relative to the read-head which could generate an apparent change in angular position. A rotary encoder system using a small encoder disk with only one read-head, is extremely sensitive to bearing wander. If an encoder disk of diameter  $d$ , moves a distance  $t$  in the direction shown in the Figure 20, due to play in the bearing, the read-head will detect movement of the graduations and indicate a counter-clockwise movement of  $t/(d/2)$  radians. For example, radial bearing wander of just  $\pm 1$  micrometres, in combination with a 50mm diameter

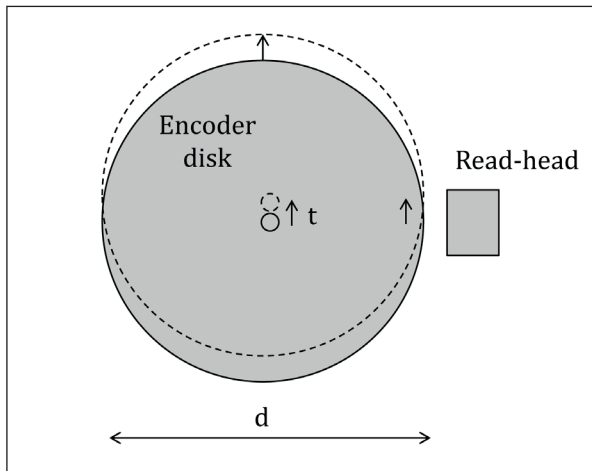


Figure 20

encoder disk, would produce a significant error of  $\pm 8.25$  arcseconds. Since bearing wander can have both repeatable and non-repeatable components, error mapping is not a technique that can be used to control this error.

To overcome this problem, the XR20 contains two diametrically opposed read-heads and the final XR20 position output is based on the average of the angular positions indicated by each read-head. Because radial bearing wander causes equal and opposite errors at each read-head the error is eliminated. This is illustrated in Figure 21. If the encoder disk again moves a distance  $t$ , read-head 1 will again indicate a counter-clockwise movement of  $t/(d/2)$  radians. But read-head 2 will indicate an equal and opposite movement of  $t/(d/2)$  radians in a clockwise direction. When the output from the two read-heads is averaged, the error is eliminated.

The use of two read-heads also conveniently removes errors due to any small off-centre mounting (see note) of the encoder disk relative to the axis of rotation of the central shaft. *Note – although the bearings and encoder disk are designed to be self centering during assembly, some eccentricity will still be present due to manufacturing tolerances.*

If the read-heads are not perfectly aligned (diametrically opposed) then the cancellation of bearing wander and eccentricity errors will not be perfect. However, because the eccentricity, bearing wander and read-head alignments within Renishaw's XR20 are kept within reasonable tolerances by the self-centering design, these second order errors can be safely ignored.

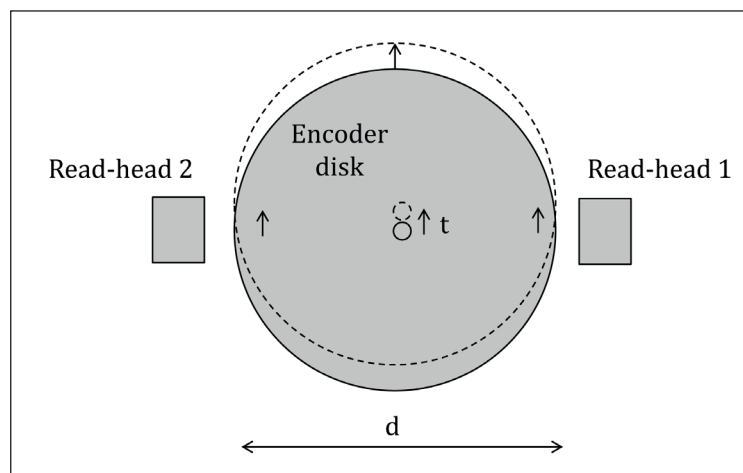


Figure 21

Note: For more detailed information on bearing wander and eccentricity errors refer to the Renishaw White Paper entitled 'The accuracy of angle encoders'.

## Graduation Errors

Now consider errors in the positions of the graduations on the encoder disk. Renishaw's manufacturing process ensures each graduation on the 50mm diameter disk is positioned within  $\pm 0.5 \mu\text{m}$ , giving an inherent angular accuracy of just over  $\pm 4$  arcseconds. Because these graduations are formed directly on the periphery of the ring they are very dimensionally stable. This, together with the absence of high frequency components, means this error can be largely eliminated by error mapping. After the XR20 has been assembled, it is calibrated using a laser interferometer system. The measured errors are stored in an internal error map which is used to correct the XR20's angular position reading when the system is in use.

$$\text{Actual position} = \text{Average read-head position} \pm \text{error map correction}$$

The error mapping process not only reduces inaccuracies due to positional errors of the graduations on the encoder ring, it also further reduces errors due to any residual misalignment ( $\alpha$ ) of the central shaft the mounting surface, misalignment ( $\omega$ ) of the retro-reflectors, and misalignments of the read-heads mentioned previously.

Note: For more detailed information on bearing wander and eccentricity errors refer to the Renishaw White Paper entitled '*The accuracy of angle encoders*'.

## Inaccuracies in the laser interferometer reading

These error sources have been covered at length in the Renishaw white paper *TE326*, so a detailed explanation is not given here, but in summary they are as follows;

### Incorrect retro-reflector spacing

The exact centre to centre spacing, between the two retro-reflectors in the angular reflector will vary depending on manufacturing tolerances and current temperature. To eliminate this error, Renishaw's Rotary axis calibration software includes a totally automatic angular optics calibration procedure which automatically identifies any error in the spacing by comparing the laser reading with the XR20 readout at  $0^\circ$ ,  $+5^\circ$  and  $-5^\circ$  positions. From these readings the software calculates a correction factor K. This procedure only takes a few seconds and is always carried out automatically, just before calibration of the axis under test starts. Subsequent angular readings from the laser are then corrected using the equation  $\theta = \arcsin(\Delta L / (K.S))$ .

The benefit of the automated calibration procedure becomes clear by considering a simple example. Suppose that, due to manufacturing tolerances, the centre to centre spacing between the two retro-reflectors in the angular reflector is 30.1mm instead of 30.0mm and suppose the interferometer is measuring an angle of  $1^\circ$ . Without correction, the error in the spacing of the retro-reflectors will cause an angular measurement error of approximately  $0.1\text{mm}/30\text{mm} \times 1^\circ = 0.0033^\circ = 12$  arcseconds. However, after the calibration routine is completed the 0.1mm error in retro-reflector spacing will be compensated for and the measurement error reduced below 0.1 arcseconds.

### Misaligned reflector at datum (i.e. not perpendicular to laser beams)

If the angular reflector is not perpendicular to the laser beam when the system is datumed, a small measurement error can occur. In addition to identifying any error in the spacing between the retro-reflectors, the automated angular optics calibration procedure (see above) also identifies any misalignment of the reflector. The XR20 is then counter-rotated accordingly to bring the reflector into perfect alignment and the system is then re-datumed before calibration of the axis under test starts, thereby eliminating this error.

### Air refractive index compensation errors

The refractive index of air, and hence the laser’s wavelength vary slightly according to the local weather conditions, but significantly according to the local altitude above sea level. When the automated angular optics calibration routine identifies any error in the spacing between the retro-reflectors (see above), the procedure uses laser readings taken under the current atmospheric conditions. Therefore the value calculated for K automatically includes a correction for air refraction errors, thereby eliminating them. Note that subsequent changes in air temperature pressure or humidity will not be compensated for. However, such errors are usually ignored since the path lengths of arms 1 and 2 of the interferometer are quite similar (and so are affected almost equally) and the subsequent refractive index change at a fixed altitude is likely to be small. For example a 1°C change in air temperature, when the interferometer and reflector are misaligned by 2.5°, will only introduce a change in reading of about 0.05 micro-radians, (0.01 arcseconds).

### Thermal expansion of angular interferometer periscope

The Renishaw white paper TE326 shows that the angular interferometer periscope optic typically has a temperature sensitivity of 13.8 micro-radians/°C (2.8 arcseconds/°C). For this reason it is wise to ensure the optics have acclimatised before the test starts, to complete the test promptly, and to minimise local variations in temperature.

### Non-parallel beams emerging from the periscope

The beams emerging from the angular periscope are guaranteed to be parallel within ±15 arcseconds. In the worst case this non-parallelism can introduce a small measurement error of ±0.5 arcseconds for every millimetre of lateral motion (i.e. at 90° to the laser beam) of the reflector. Such movement will occur if the axes of rotation of the XR20 and the axis under test are not coincident. It is therefore recommended that the system is aligned so that the two axes of rotation are coincident within ±0.5mm, thereby ensuring this error is kept below ±0.25 arcseconds.

### Practical error budgeting

It is clear that angular misalignments have the potential to create significant measurement errors and the errors combine in quite a complex manner. It is therefore important to carefully align the system and to be aware of the associated errors. Providing the XR20 is aligned and operated in accordance with the recommendations in the manual, the overall system measurement accuracy is specified to be within ±1 arcsecond.

Estimated measurement accuracy in arcseconds for various $\alpha$ and $\beta$ misalignments							
		$\alpha$ (in milli-radians)					
		0.4	1	2	3	4	5
$\beta$ in milli-radians	1	1.0	1.3	2.2	3.6	5.4	7.6
	2	1.1	1.5	2.4	3.8	5.6	7.8
	3	1.2	1.6	2.7	4.1	5.9	8.2
	4	1.3	1.8	3.0	4.5	6.4	8.7
	5	1.4	2.0	3.3	5.0	6.9	9.3

Figure 22

If achieving the alignment tolerances recommended is impractical, or if ±1 arcsecond accuracy is not required, it is possible to ‘trade-off’ larger misalignments against decreasing measurement accuracy levels. In order to simplify this process Figure 22 shows the estimated measurement accuracies that can be expected for a range of different angular misalignments.

## Off axis rotary calibration

This paper so far has concentrated on the measurement errors associated with calibrating a rotary axis with an XR20 which is mounted 'on axis', i.e. where the axes of rotation of the two systems are virtually coincident. 'On axis' mounting is often straightforward, (for example when calibrating a rotary table), making it relatively straightforward to quantify and control the misalignments  $\alpha$  and  $\beta$ .

However there are many rotary axes, especially on 4 and 5 axis machining centres, where it is difficult to access the point of rotation and where there is no convenient mounting surface, as illustrated by Figure 23. Sometimes it is possible to calibrate such axes by mounting the XR20 on a custom bracket, as illustrated in Figure 24. But such brackets may be cumbersome, difficult to align and may flex under the weight of the XR20, producing measurement errors.



Figure 23

In order to overcome this limitation, Renishaw offers an alternative solution involving synchronised movements of linear and rotary axes as illustrated in Figure 25 which shows a sequence of 3 such synchronised moves. As the rotary axis moves the linear axis supporting the angular interferometer is also moved to ensure that laser beams remain aligned. The advantage of this arrangement is that the bracket required to support the XR20 can be much more compact and rigid. The disadvantages are that a more complex part program is required and the angular data captured maybe contaminated by angular (pitch or yaw) errors in the movement of the linear axis.

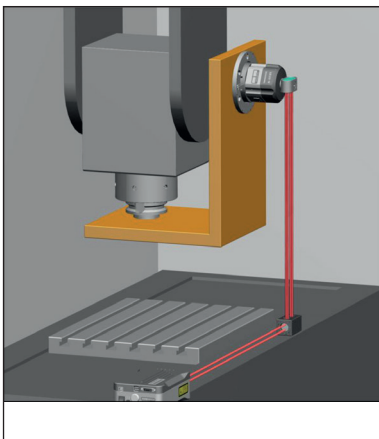


Figure 24

In order to overcome the first disadvantage Renishaw has developed special software that generates the part program automatically based on three point setup/alignment procedure.

The second disadvantage can be overcome by also measuring the angular (pitch or yaw) error in the linear axis over the short

length of travel used during the rotary axis calibration. Then, using special analysis software developed by Renishaw, the angular error recorded in the motion of the linear axis can be subtracted from the rotary calibration

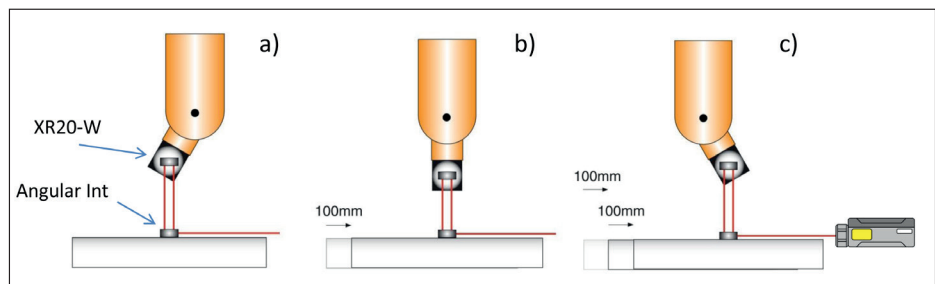


Figure 25

data before it is plotted. Alternatively, if the angular (pitch or yaw) error is checked over a longer length of the linear axis, it may be possible to select a section of the linear axis where the angular pitch or yaw error is negligible and position the angular interferometer accordingly.

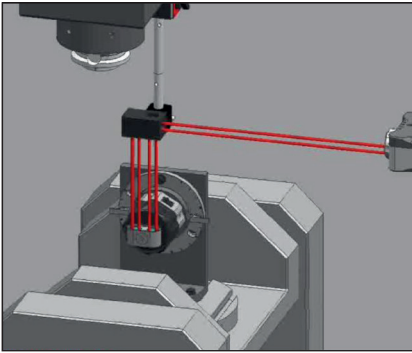


Figure 26

The same techniques can be applied to the calibration of the rotary accuracy of tilt and turn trunnion axes as shown in Figure 26. More details of this technique can be found in the 'Off axis rotary user guide' on [www.renishaw.com/lasercalsupport](http://www.renishaw.com/lasercalsupport).

## Error analysis

The errors associated with 'off axis' calibration are similar to those described previously for 'on axis' calibration, with one addition and a few important caveats.

- The 'off axis' procedure relies on correctly synchronised moves of the linear and rotary axes to maintain beam alignment. This in turn relies on a good estimate of the offsets between the axes of rotation of the XR20 and the axis under test (see Figure 27). These offsets are estimated automatically during the three point alignment setup. If arcsecond accuracy levels are required, it is important that great care is taken during this alignment process to ensure that, not only is adequate signal strength maintained at all 3 points, but also that the alignment of the beams returned to the laser is accurate. If this is not checked there is a danger that the reflector will move laterally (across the laser beam) as the test progresses. As stated earlier, under worst case conditions (an angular periscope with 15 second beam non-parallelism) a sideways movement of the reflector of  $\pm 0.5\text{mm}$  can add  $\pm 0.25$  arcseconds of measurement error.
- During 'off axis' calibration, the linear separation between the reflector and interferometer will change during the test (as illustrated in Figure 25 above). Depending on the set-up it may be difficult to ensure the laser beams, after they are turned  $90^\circ$  by the interferometer, are accurately aligned. This change in separation combined with poor alignment and the 15 arcsecond non-parallelism of the beams emerging from the interferometer can introduce an additional measurement error of up to  $\pm 0.5$  arcseconds. (The origin of this error is described in detail in sub-section entitled Non-parallel beams from angular interferometer in TE326).
- It is crucial to ensure that the sign convention of the angular data captured during the movement of the linear axis matches that of the angular data captured during the combined linear and rotary moves. Otherwise, instead of eliminating the angular errors originating from the linear axis, the subtraction process will double them!
- It is likely that the alignments achieved for  $\alpha$  and  $\beta$  when working "off axis" will not be as good as those obtained when working "on axis". As with "on-axis" calibrations, the time spent making alignment adjustments can be traded against the overall accuracy required using the table in Figure 22. However, as mentioned above, because "off axis" setups will cause a change in separation between the reflector and interferometer during the test, it is recommended that an additional measurement error of  $\pm 0.5$  arcseconds is added to the values in this table.

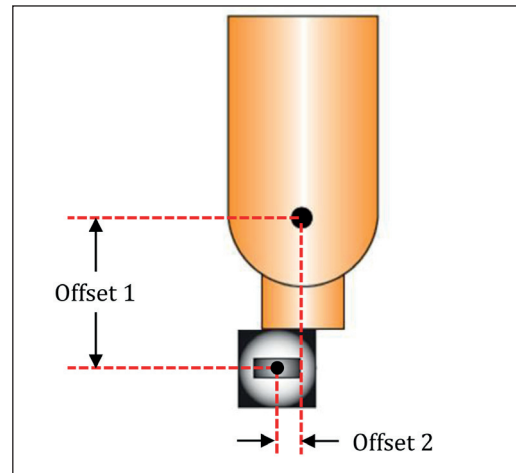


Figure 27

## Conclusion

This paper has described the operational principles and internal construction of Renishaw's XR20 Rotary Axis Calibration System. It has shown how the system can be used for both 'on axis' and 'off axis' calibration of rotary axes. The main error sources that affect the accuracy of measurement have been detailed together with how the XR20 system has been designed to minimise them. It has also provided guidance on the effect of larger alignment set-up errors on the accuracy of measurement. For further information the reader is referred to the following documents.

## References

1. Renishaw White Paper '*TE326 Interferometric angle measurement and the hardware options available from Renishaw*'.
2. Renishaw White Paper entitled '*The accuracy of angle encoders*' available on **renishaw.com**
3. Application note(s) '*Off axis rotary calibration*'



This page is intentionally left blank

**Renishaw plc**

New Mills, Wotton-under-Edge,  
Gloucestershire GL12 8JR  
United Kingdom

**T** +44 (0) 1453 524524**F** +44 (0) 1453 524901**E** uk@renishaw.com[www.renishaw.com](http://www.renishaw.com)**RENISHAW**   
apply innovation™

## About Renishaw

Renishaw is an established world leader in engineering technologies, with a strong history of innovation in product development and manufacturing. Since its formation in 1973, the company has supplied leading-edge products that increase process productivity, improve product quality and deliver cost-effective automation solutions.

A worldwide network of subsidiary companies and distributors provides exceptional service and support for its customers.

**Products include:**

- Additive manufacturing, vacuum casting, and injection moulding technologies for design, prototyping, and production applications
- Advanced material technologies with a variety of applications in multiple fields
- Dental CAD/CAM scanning and milling systems and supply of dental structures
- Encoder systems for high accuracy linear, angle and rotary position feedback
- Fixturing for CMMs (co-ordinate measuring machines) and gauging systems
- Gauging systems for comparative measurement of machined parts
- High speed laser measurement and surveying systems for use in extreme environments
- Laser and ballbar systems for performance measurement and calibration of machines
- Medical devices for neurosurgical applications
- Probe systems and software for job set-up, tool setting and inspection on CNC machine tools
- Raman spectroscopy systems for non-destructive material analysis
- Sensor systems and software for measurement on CMMs
- Styli for CMM and machine tool probe applications

For worldwide contact details, please visit our main website at [www.renishaw.com/contact](http://www.renishaw.com/contact)



RENISHAW HAS MADE CONSIDERABLE EFFORTS TO ENSURE THE CONTENT OF THIS DOCUMENT IS CORRECT AT THE DATE OF PUBLICATION BUT MAKES NO WARRANTIES OR REPRESENTATIONS REGARDING THE CONTENT. RENISHAW EXCLUDES LIABILITY, HOWSOEVER ARISING, FOR ANY INACCURACIES IN THIS DOCUMENT.

©2013 Renishaw plc. All rights reserved.

Renishaw reserves the right to change specifications without notice.

RENISHAW and the probe symbol used in the RENISHAW logo are registered trade marks of Renishaw plc in the United Kingdom and other countries. apply innovation and names and designations of other Renishaw products and technologies are trade marks of Renishaw plc or its subsidiaries. All other brand names and product names used in this document are trade names, trade marks or registered trade marks of their respective owners.



H - 5650 - 2048 - 01

Issued: 0413 Part no. H-5650-2048-01-A